

Drosophila Cep135/Bld10 maintains proper centriole structure but is dispensable for cartwheel formation

Hélio Roque, Alan Wainman, Jennifer Richens, Kasia Kozyska, Anna Franz and Jordan W. Raff*

Sir William Dunn School of Pathology, Oxford University, South Parks Road, Oxford OX1 3RE, UK

*Author for correspondence (jordan.raff@path.ox.ac.uk)

Accepted 6 August 2012

Journal of Cell Science 125, 5881–5886

© 2012. Published by The Company of Biologists Ltd

doi: 10.1242/jcs.113506

Summary

Cep135/Bld10 is a conserved centriolar protein required for the formation of the central cartwheel, an early intermediate in centriole assembly. Surprisingly, Cep135/Bld10 is not essential for centriole duplication in *Drosophila*, suggesting either that Cep135/Bld10 is not essential for cartwheel formation, or that the cartwheel is not essential for centriole assembly in flies. Using electron tomography and super-resolution microscopy we show that centrioles can form a cartwheel in the absence of Cep135/Bld10, but centriole width is increased and the cartwheel appears to disassemble over time. Using 3D structured illumination microscopy we show that Cep135/Bld10 is localized to a region between inner (SAS-6, Ana2) and outer (Asl, DSpd-2 and D-PLP) centriolar components, and the localization of all these component is subtly perturbed in the absence of Cep135/Bld10, although the ninefold symmetry of the centriole is maintained. Thus, in flies, Cep135/Bld10 is not essential for cartwheel assembly or for establishing the ninefold symmetry of centrioles; rather, it appears to stabilize the connection between inner and outer centriole components.

Key words: Bld10, Cell biology, Centrioles, Centrosomes, Cep135, *Drosophila*

Introduction

Centrioles are complex MT-based structures that form two important cell organelles: the centrosome and the cilium/flagellum. The dysfunction of these organelles is linked to several human diseases (Nigg and Raff, 2009). Surprisingly, only a small number of proteins appear to be essential for centriole duplication (Delattre et al., 2006; Dobbelaere et al., 2008; Pelletier et al., 2006). In many organisms centriole duplication is initiated by the formation of a central cartwheel, around which the centriolar MTs are assembled. In *Chlamydomonas* and *Paramecium* the centriolar protein Bld10 (Cep135 in vertebrates) is essential for cartwheel formation, and so for centriole duplication (Hiraki et al., 2007; Jerka-Dziadosz et al., 2010); Cep135 also appears to be required for efficient centriole duplication in human and *Drosophila* cells in culture (Dobbelaere et al., 2008; Kleylein-Sohn et al., 2007).

Surprisingly, flies that lack detectable Cep135/Bld10 are viable and exhibit only mild centriole defects (Blachon et al., 2009; Carvalho-Santos et al., 2010; Mottier-Pavie and Megraw, 2009). Centriole duplication and centrosome formation appeared unperturbed, and mutant flies were not uncoordinated, indicating that the sensory cilia in the type I sensory neurons (the only ciliated cells in the adult fly) were functional. In mutant spermatocytes (which normally contain larger and more elaborate centrioles than those found in other fly tissues), the centrioles were short and the flagellar axonemes often lacked the central pair of MTs, rendering the sperm immotile. Otherwise, however, the flagellar axoneme appeared structurally normal. These findings present something of a paradox, as they suggest that either Cep135/Bld10 is not essential for cartwheel formation, or that the cartwheel is not an essential intermediate in centriole assembly. Here we use electron tomography (ET) and super

resolution 3D structured illumination microscopy (3D-SIM) to investigate the role of *Drosophila* Cep135/Bld10 *in vivo*.

Results

Cep135 mutant spermatocyte centrioles have defective cartwheels

To test whether a lack of Cep135/Bld10 affects the cartwheel structure in *Drosophila* we used electron tomography (ET) to examine centrioles in WT mature primary spermatocytes. These cells contain large centrioles that form short cilia (Fuller, 1993; Tate, 1971). Our ET analysis of WT cells revealed a complex organization of the centriole/cilia. In all centriole pairs examined ($n=8$; 16 centrioles in total), mothers (recognized because daughter centrioles were abutted to their outer walls) and daughters invariably had a short central cartwheel at their proximal end (Fig. 1A–C, brackets; supplementary material Movies 1–3). After a short gap there were then usually 1–3 more electron-dense regions above the cartwheel (Fig. 1A–C, arrowheads); we shall refer to this region as the intermedial zone. In all mothers, and in the longer (presumably more mature) daughters, a well defined ‘central tube’ was present just above the intermedial zone that extended distally (Fig. 1A,B, arrows). The length of the central tube was variable: in some cases it extended all the way into the cilia, and in two cases a second central tube was formed in close proximity to the first tube (supplementary material Fig. S1A,B). In shorter (presumably less mature) daughters no well defined central tube was visible (Fig. 1C, open arrows).

It has previously been shown that Cep135/Bld10 protein is undetectable in *Cep135*^{c04199} mutant cells by immunofluorescence and western blotting (Blachon et al., 2009; Carvalho-Santos et al., 2010; Mottier-Pavie and Megraw, 2009) and we confirmed that

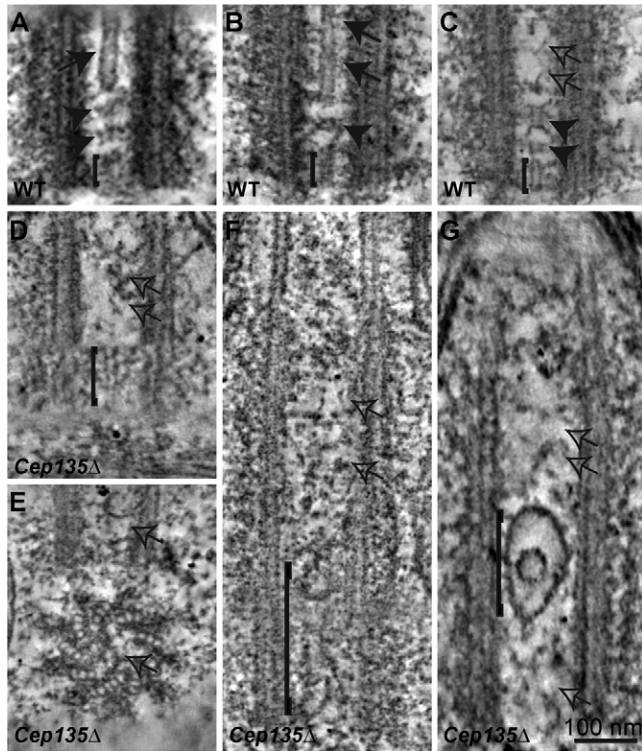


Fig. 1. Cep135 is required for cartwheel and central tubule stability. Electron tomogram (ET) analysis of WT mother (A) and daughter (B) centriole showing the proximal central cartwheel (bracket), the intermedial zone above it (arrowheads) and the prominent central tube that extends towards the distal end of the centriole (arrows). (C) A WT daughter centriole where the cartwheel (bracket) and intermedial zone (arrowheads) are present, but no central tube has yet formed (open arrows). (D) A *Cep135Δ* daughter centriole that contains a cartwheel (bracket), but where no transition zone or central tube is visible (open arrows). (E) A *Cep135Δ* centriole pair where no cartwheel structure is recognizable in either centriole (open arrows). (F) A *Cep135Δ* daughter centriole with a deformed tube-like structure at the proximal end (bracket). No other structures are visible (open arrows). (G) A *Cep135Δ* mother centriole that lacks a recognizable cartwheel, but has an unusual structure in its middle (bracket). All images are single planes of a tomogram (and hereafter) and are shown at the same scale. Note that only the proximal ends of the WT centrioles are shown in A–C, while more extended views of some of the mutant centrioles and cilia are shown (F,G).

this was the case (data not shown). Importantly, the centriole defects we describe below in primary spermatocytes were rescued by the co-expression of a single RFP-Cep135 transgene in the *Cep135* mutant (hereafter *Cep135Δ*) background (supplementary material Fig. S1C).

In *Cep135Δ* mature primary spermatocytes centrioles exhibited clear central cartwheel defects. From five centriole pairs acquired (10 centrioles in total) only two daughters had a clear cartwheel (Fig. 1D, bracket; supplementary material Movie 4). Seven of the other eight centrioles (four mothers and three daughters) had no clear cartwheel (Fig. 1E, open arrows; supplementary material Movie 5) while one mother had a defective cartwheel that was undulating and misshapen (Fig. 1F, bracket; supplementary material Movie 6). An abnormal spherical structure was visible in the center of one the centrioles that lacked a cartwheel (Fig. 1G, square bracket; supplementary material Movie 7). Strikingly, none of the mutant

centrioles contained a detectable central tube (Fig. 1D–G, open arrows). Nevertheless, when viewed in cross section, the structure and ninefold symmetry of the centriolar MT blades appeared unperturbed (Fig. 1E). Thus, *Cep135/Bld10* is not essential for cartwheel formation in fly spermatocytes, but cartwheels appear unstable in its absence, and the elongating centrioles appear unable to assemble a central tube.

***Cep135Δ* cartwheel defects are milder in younger centrioles**

We next examined centrioles at earlier stages of primary spermatocyte development, before they had migrated to the cell surface to form cilia. In WT centrioles ($n=7$ pairs, 14 centrioles in total) a cartwheel was observed in all mother and daughter centrioles (Fig. 2A, arrow and brackets; supplementary material Movie 8). In *Cep135Δ* centrioles ($n=8$ pairs, 16 centrioles in total) all mothers appeared to lack cartwheels (Fig. 2B, open arrowhead) but all daughters appeared to have cartwheels (Fig. 2B, bracket; supplementary material Movie 9). A careful analysis of the mother centrioles along their entire length, however, revealed that a cartwheel-like structure was detectable in some transverse sections (Fig. 2C, filled arrowheads in red, blue and yellow boxed panels), but not others (Fig. 2C, open arrowhead, green boxed panel). These structures were often displaced from the center of the centriole, suggesting that they were not properly connected to the outer centriolar MT blades. We conclude that residual cartwheel-like structures are present in at least some of these mutant centrioles even when no clear structure can be seen in a longitudinal view. These data suggest that relatively normal cartwheels are initially formed in daughter centrioles, but these appear to deteriorate over time and are more disorganized in mother centrioles.

It has previously been shown that the centrioles in *Cep135Δ* spermatocytes are shorter than normal, and our ET data confirmed that this was the case (supplementary material Fig. S1D,E). In addition, we found that although the diameter of the central hub of the cartwheel appeared unaffected in *Cep135Δ* centrioles (data acquired from all centrioles where a clear cartwheel structure could be identified, Fig. 2D) mutant centrioles were wider than normal (data acquired from all centrioles whether they had a cartwheel or not, Fig. 2E). These data suggest that *Cep135/Bld10* is not required for cartwheel formation, but rather is required to properly connect the cartwheel to the outer centriolar structures: in its absence this connection is not maintained properly and the diameter of the centriole increases.

The localization of inner and outer centriole components is disrupted in *Cep135Δ* centrioles

To address how the structural changes we observe in *Cep135Δ* centrioles might translate into molecular changes we used 3D-SIM to examine the localization of GFP-fusions to two components of the *Drosophila* cartwheel, DSas-6 and Ana2 (Stevens et al., 2010b), and of endogenous Asl, a protein known to localize to the outer wall of the centriole (Blachon et al., 2009; Sir et al., 2011; Varmark et al., 2007). In WT centrioles Asl formed a tube with an average diameter of 299 ± 30.7 nm (Fig. 2F,G); from our ET analysis the average diameter of the centrioles from the edge of the outer MT of the centriole triplets was 199 ± 12.6 nm (data not shown), supporting the conclusion that Asl is concentrated in a region just outside the MT triplets. GFP-DSas-6 and Ana2-GFP both formed extended ‘fibers’

(sometimes beaded in appearance) that were located at both the proximal and distal ends of the centriole within the Asl tube; intriguingly, both proteins also often formed a fiber that appeared to extend distally from the Asl tube (Fig. 2F). By comparing length measurements between these 3D-SIM images and our ET images (supplementary material Fig. S1F), it seems likely that the Asl tube surrounds the entire centriole/basal body structure, and that the distal GFP-DSas-6 and Ana2-GFP fibers extend into the small cilia. Unfortunately, the optical resolution of the 3D-SIM images does not allow us to resolve whether these structures are tubes (rather than fibers) but it seems likely that they correspond to the cartwheel, intermediary zone and central tube structures that we observed by ET.

We observed a range of defects in the localization of these proteins in *Cep135Δ* spermatocytes. In some cases a relatively normal Asl tube was present, but the localization of GFP-DSas-6 and Ana2-GFP was perturbed: both proteins still occasionally formed extended fibers, but sometimes these fibers were missing, and very often the proteins exhibited a much-less extended and more dot-like appearance, with the dots often being unevenly distributed within the lumen of the centriole (Fig. 2F). Most surprisingly, we also often observed that the Asl staining was disrupted; indeed, even in some centrioles with relatively well defined GFP-DSas-6 or Ana2-GFP fibers, the Asl tube was

clearly perturbed. Moreover, the diameter of the Asl tube (when it was present) was wider in *Cep135Δ* spermatocytes, supporting our conclusion from the ET data that centrioles are wider in the absence of Cep135/Bld10 (Fig. 2F,G). Thus, the distribution of both inner and outer centriole components is subtly perturbed in the absence of Cep135/Bld10.

Centriole structure is perturbed in *Cep135Δ* wing disc centrioles

The centrioles in primary spermatocytes are much larger and more elaborate than those found in most other *Drosophila* tissues (González et al., 1998). To see if the defects we observed in *Cep135Δ* spermatocyte centrioles were also found in more ‘typical’ *Drosophila* centrioles we used TEM and ET to examine the centrioles in imaginal wing discs of 3rd instar larvae. As in spermatocytes, the centrioles in *Cep135Δ* were shorter (WT=126±2.66 nm, *n*=42; *Cep135Δ*=109±4.79 nm, *n*=34; *P*=0.0017) and wider in both inner (WT=78.6±1.38 nm, *n*=36; *Cep135Δ*=92.60±5.67 nm, *n*=30; *P*=0.0163) and outer diameter (WT=185.5±2.73 nm, *n*=37; *Cep135Δ*=203.3±5.15 nm, *n*=33; *P*=0.0043) (supplementary material Fig. S2A). In all WT centrioles (*n*=10 pairs and one single centriole, 21 in total) the cartwheel extended the whole length of the centriole (Fig. 3A, arrowhead and brackets; supplementary material Movie 10). In all *Cep135Δ* centrioles (*n*=12 pairs and 3 single centrioles, 27 in total) a central cartwheel was detectable, but in 10/12 mothers the cartwheel structure was perturbed with most (7/10) having an abnormally undulating appearance (Fig. 3B, arrowhead left panel, brackets right panel; supplementary material Movie 11) and the rest (3/10) having only remnants of a cartwheel structure observable in some tangential sections. As in spermatocytes, the inner centriole diameter was also enlarged (Fig. 3C), and this was true for both mothers and daughters, indicating that, even when a cartwheel is

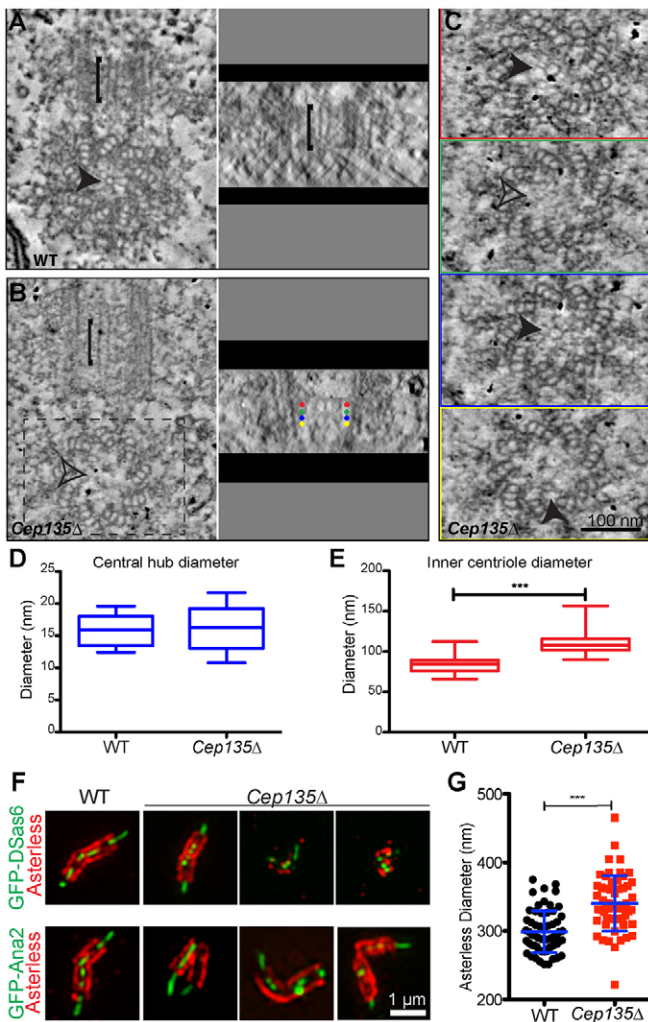


Fig. 2. Spermatocyte centriolar structure is disrupted in the absence of Cep135. Analysis of a centriole pair from a young WT (A) or young *cep135Δ* (B) primary spermatocyte where the centrioles have not yet started to elongate. Left panels show the mother centrioles in cross section and the daughter centrioles in longitudinal section; right panels show a longitudinal section of the same mother centriole (derived from the tomogram). In the WT cell, both mother and daughter centrioles have a cartwheel (bracket and arrowhead). In the *Cep135Δ* cell, the daughter centriole has a cartwheel (bracket), but no clear cartwheel is present in the mother (open arrowhead in cross section view; colored dots in longitudinal view). (C) A cross section view of the same mother centriole shown in B at various lengths along the centriole – colored boxes correspond to the position of the colored dots in B. A cartwheel-like structure is present in some sections (arrowheads), but this varies in size and position within the centriole. In some sections, no cartwheel is detectable (open arrowhead). Images (A,B,C) are shown at the same scale. (D) The box plot shows the distribution of central hub diameters from WT spermatocyte centrioles (*n*=28) and from *Cep135Δ* spermatocyte centrioles that contained a cartwheel (*n*=11). (E) The box plot shows the distribution of the inner centriole diameters in spermatocytes from WT (*n*=28) centrioles and from *Cep135Δ* centrioles (whether they contained a cartwheel or not) (*n*=26); The *Cep135Δ* centrioles are significantly wider than WT (***P*<0.0001). In this, and all subsequent box plots, the box indicates the mean, 25% and 75% percentiles, while the whiskers indicate minimum and maximum values. (F) 3D-SIM representative images of WT and *Cep135Δ* centrioles from mature primary spermatocytes. All 3D-SIM images are maximum intensity projections of 3D stacks. (G) Distribution of the Asl tube diameter as visualized by 3D-SIM for WT and *Cep135Δ* centrioles. Blue lines indicate mean and s.d. (***P*<0.0001, *n*=60 and 57 for WT and *Cep135Δ*, respectively).

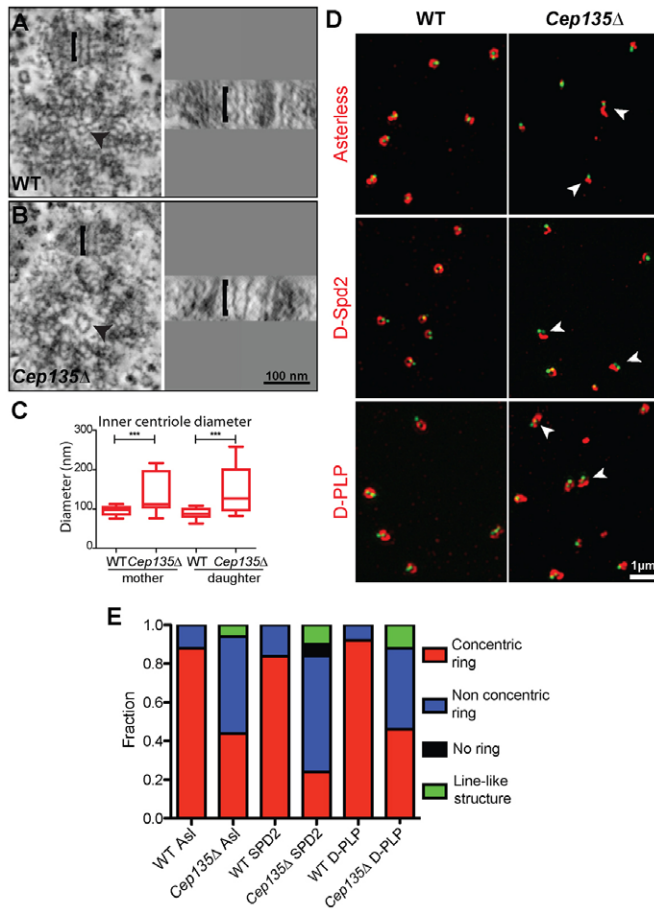


Fig. 3. The organization of both the inner and outer centriole regions is disrupted in *Cep135Δ* somatic cells. (A,B) A centriole pair from WT (A) or *Cep135Δ* (B) wing discs (A,B) (displayed as described in Fig. 2). All the centrioles have a cartwheel structure (brackets and arrowheads), but the *Cep135Δ* mother centriole in wing discs (B) has a deformed central hub: compare right panels of A and B. (C) The box plots show the diameter of the inner centriole in mother and daughter centrioles in WT and *Cep135Δ* wing disc cells. The inner centriole diameter is significantly larger in both mother and daughter *Cep135Δ* centrioles in the wing discs ($***P < 0.0001$, $n = 10$ for mother and daughter WT centrioles and 12 for mother and daughter *Cep135Δ* centrioles). (D) 3D-SIM images of wing disc centrioles revealed by GFP-DSas6 (green) in WT (left panels) and *Cep135Δ* (right panels) that have been co-stained for either endogenous Asl, D-Spd-2 or D-PLP (red – as indicated). Both single and centriole pairs are visible. Arrowheads highlight centrioles where the outer centriolar proteins (red) appear disorganized in *Cep135Δ* cells. (E) Quantification of the localization defects for Asl, D-Spd-2 and D-PLP in *Cep135Δ* wing disc centrioles ($n = 50$ centriole pairs for each genotype).

present, the centrioles are wider than normal. We conclude that the function of Cep135/Bld10 in maintaining the cartwheel structure and influencing the width of the centrioles is not restricted to the more elaborate spermatocyte centrioles.

We also analyzed WT and *Cep135Δ* wing disc centrioles by 3D-SIM. In WT centrioles GFP-DSas-6 and Ana2-GFP were usually concentrated in one or two closely associated dots (Fig. 3D; supplementary material Fig. S2B), only one of which – presumably the mother centriole (Sir et al., 2011) – was surrounded by a ring of Asl (Fig. 3D). In *Cep135Δ* centrioles, we could detect no difference in the dot-like localization of either

GFP-DSas-6 of Ana2-GFP (Fig. 3D; supplementary material Fig. S2B). Intriguingly, however, the Asl ring surrounding one of the centrioles was often not as well organized in *Cep135Δ* cells (Fig. 3D,E), and this was also the case for two other centriolar proteins that are concentrated in the more outer regions of the centriole, D-Spd-2 and D-PLP (the *Drosophila* homolog of Pericentrin) (Fig. 3D,E). Thus, as in spermatocytes, the molecular organization of the outer region of the centrioles is perturbed in these wing disc centrioles.

Cep135Δ embryo centrioles all have cartwheels

To further test our hypothesis that cartwheel structures are initially formed normally in the absence of Cep135/Bld10 but then deteriorate over time, we used ET to examine centrioles in early embryos, where the rapid cell cycle time means that all of the centrioles are no more than a few hours old. We could detect no obvious defect in cartwheel structure in *Cep135Δ* embryo centrioles compared to WT ($n = 10$ centrioles for each genotype) (Fig. 4A,B), although the diameter of the inner centriole was slightly enlarged in the absence of Cep135/Bld10, indicating that these centrioles were not entirely normal even when only a few hours old (Fig. 4C). These findings strongly support our hypothesis that in *Cep135Δ* centrioles the cartwheel degenerates with age.

The localization of Cep135/Bld10 in *Drosophila* centrioles

Immunoelectron microscopy (EM) studies have shown that Bld10 localizes primarily to the outer region of the central cartwheel spokes in *Chlamydomonas* and *Paramecium* (Hiraki

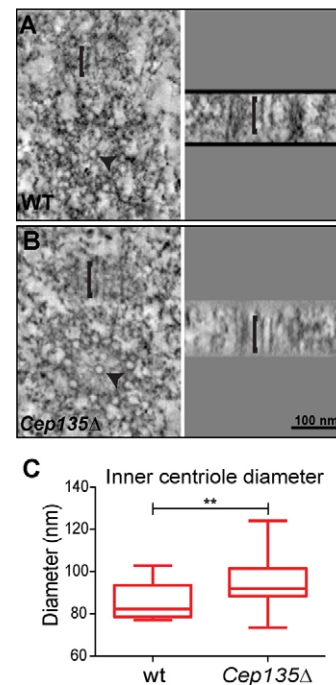


Fig. 4. *Cep135Δ* embryonic centrioles have cartwheels but are wider than normal. ET analysis of an embryo centriole pair from WT (A) or *Cep135Δ* (B) (displayed as described in Fig. 2); the cartwheel structure (brackets and arrowheads) is visible in all centrioles. (C) The box plots show the diameter of the inner centriole in wild type (wt) and *Cep135Δ* embryo cells. The inner centriole diameter is significantly larger in *Cep135Δ* centrioles; ($**P < 0.001$, $n = 10$ for each genotype).

et al., 2007; Jerka-Dziadosz et al., 2010), and to the lumen of the centriole in *Drosophila* spermatocytes (Mottier-Pavie and Megraw, 2009) and cultured human cells (although a small fraction could also be detected in the outer wall of the centriole in human cells) (Kleylein-Sohn et al., 2007). We examined the localization of *Drosophila* Cep135 protein in wingdiscs using immuno-EM and confirmed that it localized primarily to the lumen of the centriole while Asl was predominantly localized to the outer region of the centriole (supplementary material Fig. S2C–E). Using 3D-SIM we showed that GFP-Cep135 was localized within the centriolar wall defined by the Asl staining, but slightly outside the inner cartwheel structure defined by the GFP-DSas-6 and Ana2-GFP staining (Fig. 5A,B), thus positioning the protein between the inner and outer regions of the centriole. Intriguingly, in wing disc mother centrioles the GFP-Cep135 appeared to form a ring-like structure just inside the Asl ring, while a small ‘cup’ of staining could be seen outside the Asl tube, presumably reflecting the presence of some GFP-Cep135 in the region of the newly formed daughter centriole.

Discussion

Taken together our results suggest that, unlike in *Chlamydomonas* and *Paramecium*, Cep135/Bld10 is not essential for cartwheel formation in *Drosophila*. Instead,

Cep135/Bld10 appears to function to stabilize the cartwheel and the interaction between the cartwheel and the more outer regions of the centrioles. In the absence of Cep135/Bld10 cartwheels are initially formed relatively normally but they then appear to deteriorate over time. Cartwheels are often displaced from the center of the centriole, the diameter of the centriole is increased, and the localization of both inner and outer centriolar components is subtly perturbed. These phenotypes are in good agreement with our localization studies that show Cep135/Bld10 localizing to a region between the inner and outer regions of the centriole.

It has previously been shown that *Drosophila* Cep135/Bld10 is essential for the formation of the central pair of MTs in the flagellar axoneme (Carvalho-Santos et al., 2010; Mottier-Pavie and Megraw, 2009), and we show that it is also essential for the formation of a central tube structure that often extends into the short cilia formed in mature primary spermatocytes (a structure first observed by Bates, 1971). This central tube could be a MT, although our 3D-SIM analyses indicate that the cartwheel components DSas-6 and Ana2 localize to this structure. An important caveat to this result is that both of these proteins are overexpressed in these experiments compared to the endogenous proteins, so they could be binding to this structure when they would not normally do so. Nevertheless, it seems reasonable to conclude that this structure is either not a MT (and is in some way related to the central tube of the cartwheel), or is a specialized MT that is capable of binding overexpressed DSas-6 and Ana2 (while other MTs in the centriole do not). How the formation of the central tube in these centrioles and cilia might relate to the formation of the central pair of MTs in the flagellar axoneme is unclear, but it is intriguing that the formation of both structures requires Cep135/Bld10. Perhaps the central tube present in the centrioles is in some way required for the eventual growth of the central pair of MTs in the flagellar axoneme.

Materials and Methods

Fly stocks, antibodies and immunofluorescence

Fly stocks used in this study were described previously: wild-type *Oregon R*, GFP-Sas6 (Peel et al., 2007), GFP-Ana2 (Stevens et al., 2010a), and *bld10^{e04199}* (*Cep135Δ*) (Mottier-Pavie and Megraw, 2009). All mutant tissues analyzed were both maternally and zygotically mutant (i.e. they were taken from homozygous mutants derived from homozygous mutant mothers) with the exception of mature adult testes, where the testes were taken from flies derived from a mixture of homozygous and heterozygous females. All transgenic lines generated here expressed GFP- or RFP-fusions of Cep135/Bld10 under the control of the Ubiquitin promoter, which drives expression at moderate levels in all tissues (Lee et al., 1988). For immunofluorescence analysis we used the following antibodies: Rabbit anti-Cep135 (this study – raised against amino acids 401–700 of the *Drosophila* Cep135/Bld10 coding sequence); Guinea-Pig anti-Asl (this study – raised against amino acids 1–333 of Asterless coding sequence); Rabbit anti-Cnn (Lucas and Raff, 2007). Secondary antibodies used were Alexa 488 anti-Rabbit and Alexa 568 anti-Guinea Pig. Testes of adult flies were dissected and fixed as previously described (Dix and Raff, 2007). Testes were imaged on an Olympus Fluoview FV1000 with a 100×/1.40 Oil UPlanSApo objective. Images were processed and centrioles measured using ImageJ.

Sample preparation, electron tomography and immuno-electron microscopy

Sample preparation for testes was previously described (Stevens et al., 2010b). Wing-discs from 3rd instar larvae were dissected in PBS and prepared similarly to testes. Embryos were collected in fruit juice plates for 1 h and aged for 1 h. Early syncytial embryos were processed as previously described (Dzhindzhev et al., 2010). Immunolabeling and electron tomography were performed as previously described (Stevens et al., 2010b). Primary antibodies for immunolabeling were Rabbit anti-Asterless (Stevens et al., 2009) or Rabbit anti-Cep135 (this study). The secondary antibody used was 10 nm Gold Conjugated Goat Anti-Rabbit (Invitrogen). Tilt-series were acquired using SerialEM (Mastrorade, 2005) and tomograms reconstructed using the IMOD package (Kremer et al., 1996).

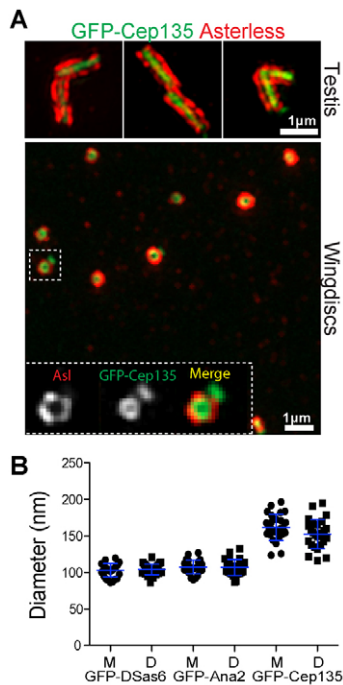


Fig. 5. Cep135 is concentrated between the cartwheel and the outer wall of the centrioles. (A) 3D-SIM images depicting the distribution of GFP-Cep135 (green) and Asterless (red) in adult primary spermatocytes (upper panels) and wing disc cells (lower panel). The inset in the lower panel shows a magnified view of the marked area with each label shown in monochrome and a merged view. (B) Diameter distribution of several GFP proteins in mother (M) and daughter (D) centrioles of adult primary spermatocytes showing that GFP-Cep135 ($n=26$ centriole pairs) localizes to a wider area than GFP-DSas6 ($n=28$ centriole pairs) or GFP-Ana2 ($n=25$ centriole pairs). Blue lines indicate mean and s.d.

3D-structured illumination microscopy

Samples of testis and wingdiscs of 3rd instar larvae were prepared for 3D-SIM similarly to preparation for immunofluorescence with minor alterations. Testes and wingdiscs were squashed onto coverslips and fixed. The antibodies used were Rabbit anti-Asl (Stevens et al., 2009), Rabbit anti-DSpd2 (Dix and Raff, 2007), Rabbit anti-PLP (Martinez-Campos et al., 2004). Secondary antibodies used were Alexa 590 anti-Rabbit (Invitrogen) and GFP-Booster (Chromotek). Image stacks for super-resolution imaging were acquired in an OMX microscope (Applied Precision) with a 100 \times , 1.4 NA oil objective (Olympus) and processed using SoftWorx software (Applied Precision).

Data analysis

GFP protein diameters were measured by fitting a Gaussian to the profile intensity and extracting the Full Width Half Maximum value. Asterless tube diameters were measured by fitting a Double Gaussian curve to the intensity profile and measuring the distance between both peaks. Fitting was done using Prism 5d software (GraphPad). Distributions were tested for Gaussian distributions by the D'Agostino & Pearson omnibus test. Significance between distributions was tested by an unpaired *t* test for Gaussian distributions and the Mann–Whitney test for non-Gaussian distributions.

Acknowledgements

We thank members of the Raff lab for advice and comments on the manuscript, and the Micron Oxford Advanced Bioimaging Unit for access to the OMX system.

Funding

This work was funded by a Cancer Research UK program grant [grant number C5395/A10530 to H.R., A.W., J.R., A.F., and J.W.R.]; and a Wellcome Trust PhD programme studentship [grant number 097297/Z/11/Z to K.K.]. Deposited in PMC for release after 6 months.

Supplementary material available online at

<http://jcs.biologists.org/lookup/suppl/doi:10.1242/jcs.113506/-/DC1>

References

- Blachon, S., Cai, X., Roberts, K. A., Yang, K., Polyanovsky, A., Church, A. and Avidor-Reiss, T. (2009). A proximal centriole-like structure is present in *Drosophila* spermatids and can serve as a model to study centriole duplication. *Genetics* **182**, 133–144.
- Carvalho-Santos, Z., Machado, P., Branco, P., Tavares-Cadete, F., Rodrigues-Martins, A., Pereira-Leal, J. B. and Bettencourt-Dias, M. (2010). Stepwise evolution of the centriole-assembly pathway. *J. Cell Sci.* **123**, 1414–1426.
- Delattre, M., Canard, C. and Gönczy, P. (2006). Sequential protein recruitment in *C. elegans* centriole formation. *Curr. Biol.* **16**, 1844–1849.
- Dix, C. I. and Raff, J. W. (2007). *Drosophila* Spd-2 recruits PCM to the sperm centriole, but is dispensable for centriole duplication. *Curr. Biol.* **17**, 1759–1764.
- Dobbelaere, J., Josué, F., Suijkerbuijk, S., Baum, B., Tapon, N. and Raff, J. (2008). A genome-wide RNAi screen to dissect centriole duplication and centrosome maturation in *Drosophila*. *PLoS Biol.* **6**, e224.
- Dzhindzhev, N. S., Yu, Q. D., Weiskopf, K., Tzolovsky, G., Cunha-Ferreira, I., Riparbelli, M., Rodrigues-Martins, A., Bettencourt-Dias, M., Callaini, G. and Glover, D. M. (2010). Asterless is a scaffold for the onset of centriole assembly. *Nature* **467**, 714–718.
- Fuller, M. T. (1993). Spermatogenesis. In *The Development of Drosophila* (ed. M. Martinez-Arias and M. Bate), pp. 71–147. Cold Spring Harbor, NY: Cold Spring Harbor Press.
- González, C., Tavasolis, G. and Mollinari, C. (1998). Centrosomes and microtubule organisation during *Drosophila* development. *J. Cell Sci.* **111**, 2697–2706.
- Hiraki, M., Nakazawa, Y., Kamiya, R. and Hirono, M. (2007). Bld10p constitutes the cartwheel-spoke tip and stabilizes the 9-fold symmetry of the centriole. *Curr. Biol.* **17**, 1778–1783.
- Jerka-Dziadosz, M., Gogendeau, D., Klotz, C., Cohen, J., Beisson, J. and Koll, F. (2010). Basal body duplication in *Paramecium*: The key role of Bld10 in assembly and stability of the cartwheel. *Cytoskeleton*, **67**, 161–171.
- Kleylein-Sohn, J., Westendorf, J., Le Clech, M., Habedanck, R., Stierhof, Y.-D. and Nigg, E. A. (2007). Plk4-induced centriole biogenesis in human cells. *Dev. Cell* **13**, 190–202.
- Kremer, J. R., Mastronarde, D. N. and McIntosh, J. R. (1996). Computer visualization of three-dimensional image data using IMOD. *J. Struct. Biol.* **116**, 71–76.
- Lee, H. S., Simon, J. A. and Lis, J. T. (1988). Structure and expression of ubiquitin genes of *Drosophila melanogaster*. *Mol. Cell Biol.* **8**, 4727–4735.
- Lucas, E. P. and Raff, J. W. (2007). Maintaining the proper connection between the centrioles and the pericentriolar matrix requires *Drosophila* centrosomin. *J. Cell Biol.* **178**, 725–732.
- Martinez-Campos, M., Basto, R., Baker, J., Kernan, M. and Raff, J. W. (2004). The *Drosophila* pericentriolar protein is essential for cilia/flagella function, but appears to be dispensable for mitosis. *J. Cell Biol.* **165**, 673–683.
- Mastronarde, D. N. (2005). Automated electron microscope tomography using robust prediction of specimen movements. *J. Struct. Biol.* **152**, 36–51.
- Mottier-Pavie, V. and Megraw, T. L. (2009). *Drosophila* bld10 is a centriolar protein that regulates centriole, basal body, and motile cilium assembly. *Mol. Biol. Cell* **20**, 2605–2614.
- Nigg, E. A. and Raff, J. W. (2009). Centrioles, centrosomes, and cilia in health and disease. *Cell* **139**, 663–678.
- Peel, N., Stevens, N. R., Basto, R. and Raff, J. W. (2007). Overexpressing centriole-replication proteins in vivo induces centriole overduplication and de novo formation. *Curr. Biol.* **17**, 834–843.
- Pelletier, L., O'Toole, E., Schwager, A., Hyman, A. A. and Müller-Reichert, T. (2006). Centriole assembly in *Caenorhabditis elegans*. *Nature* **444**, 619–623.
- Sir, J. H., Barr, A. R., Nicholas, A. K., Carvalho, O. P., Khurshid, M., Sossick, A., Reichelt, S., D'Santos, C., Woods, C. G. and Gergely, F. (2011). A primary microcephaly protein complex forms a ring around parental centrioles. *Nat. Genet.* **43**, 1147–1153.
- Stevens, N. R., Dobbelaere, J., Wainman, A., Gergely, F. and Raff, J. W. (2009). Ana3 is a conserved protein required for the structural integrity of centrioles and basal bodies. *J. Cell Biol.* **187**, 355–363.
- Stevens, N. R., Dobbelaere, J., Brunk, K., Franz, A. and Raff, J. W. (2010a). *Drosophila* Ana2 is a conserved centriole duplication factor. *J. Cell Biol.* **188**, 313–323.
- Stevens, N. R., Roque, H. and Raff, J. W. (2010b). DSas-6 and Ana2 coassemble into tubules to promote centriole duplication and engagement. *Dev. Cell* **19**, 913–919.
- Tates, A. D. (1971). Cytodifferentiation during spermatogenesis in *Drosophila melanogaster*. Vol. Doctor. Leiden, The Netherlands: Leiden University.
- Varmark, H., Llamazares, S., Rebollo, E., Lange, B., Reina, J., Schwarz, H. and Gonzalez, C. (2007). Asterless is a centriolar protein required for centrosome function and embryo development in *Drosophila*. *Curr. Biol.* **17**, 1735–1745.